CN2

Compensation of Magnetic Saturation of Self-sensing Magnetic Levitation *

Kohei MATSUDA**, Tetsuzo SAKAMOTO***

Abstract

This paper investigates the magnetic saturation problem of self-sensing electromagnetic levitation system and presents a novel self-sensing scheme. The proposed approach employs a demodulation technique. By superimposing a high frequency voltage, the resulting electromagnet coil currents have ripples that can be used for gap sensing. This paper shows the effect of magnetic saturation on the gap sensing and the gap length is not uniquely determined when using the relation between the ripple, control current and the gap in simulations. The results imply that the constraint conditions are to be determined to solve the problem. The proposed approach utilizes the dynamical motion model of the electromagnetic levitation system to uniquely identify the gap. By using the system behavior information, the gap can be uniquely estimated. To incorporate the dynamical model with the gap sensing algorithm, the unscented Kalman filter is employed. The proposed estimator is demonstrated in simulations. The results show that it is possible to deal with magnetic saturation by using the proposed gap sensing scheme. The estimator has a good accuracy in wide gap range compared to the conventional method.

Key words: self-sensing, senorless, electromagnetic levitation, magnetic saturation, position estimation, unscented Kalman filter

1. Introduction

Magnetic levitation technology provides a frictionless feature. This system is employed for some applications such as magnetic bearings, turbo machines, and magnetically levitated vehicles. The electromagnetic suspension system is inherently unstable and needs to be controlled. In most of cases, the stabilization is achieved with a displacement sensor that detects the position of the suspended object. The electromagnetic levitation which eliminates the position sensors and estimates the potion from the currents in the electromagnet is called the self-sensing electromagnetic levitation. The self-sensing technique is preferable in terms of the cost and reliability of the system. Additionally simplification of the mechanism and sensor/actuator collocation are achievable.

The self-sensing approaches are to design an algorithm that transduces the voltage and current into the position signal. There are some approaches. One of the method is the state estimation approach and was first proposed by Visher[1]. A one-degree of freedom electromagnetic levitation system can be modeled by a single-input single-output linear time invariant model. The model is controllable and observable. A linear state observer can be used for the estimation of the gap from the voltage and current. By using the estimated gap, the object can be suspended. However the model has a non-minimum phase zero and an unstable pole. This characteristic represents a poor robustness of the self-sensing electromagnetic levitation system. Some researchers investigated the limitation of the robustness[2) 3) 4)]. One of the alternative methods are the amplitude modulation approach. Many researchers have studied self-sensing techniques uisng this approach[5) 6) 7) 8)]. The approach is based on measuring the inductance, which utilizes a high frequency voltage input to prevent mutual interference with the control voltage. The sum of the high frequency voltage and the control voltage is applied to the coil. Then the excited coil current has ripple components from which the gap length can be calculated. The robustness of this self-sensing system is analyzed by the linear periodic system framework [9) 10)]. The papers[9) 10)] showed that the robustness of the system improves by injecting high frequency voltage to the coil. Although the modulation approach is not a new idea, it still remains a technical challenge.

One of the major problems associated with the self-sensing technique to be addressed is the magnetic saturation. Since the nonlinear phenomenon of magnetic materials influences the self-inductance of the coil, the accuracy of the gap estimation is deteriorated. For this magnetic saturation problem, some researchers presented the compensation methods[11) 12) 13) 14)]. However, these methods are only valid for applications such as magnetic bearing. It is not clear that the validation of these self-sensing schemes can be ensured in the wide air gap range.

In this paper, we investigate the magnetic saturation problem of self-sensing electromagnetic levitation and present a new self-sensing scheme. The proposed scheme employs an amplitude demodulation technique. In the section 3, we show static self-sensing characteristics to confirm the influence by magnetic saturation. And we shows that the gap is not uniquely determined by using the relation among the ripple, control current and the gap. To uniquely identify the air gap length, the proposed scheme

*

** Graduate School of Engineering, Graduate School, Kyushu Institute of Technology (1-1,Sensui-cho, Tobata, Kitakyushu, Fukuoka, 804-8550, Japan)

*** Facaulty of Engineering, Gradutae School, Kyushu Institute of Technology (1-1 Sensui-cho, Tobata, Kitakyushu, Fukuoka, 804-8550, Japan)

utilizes the dynamical model of the electromagnetic levitation system. To incorporate the system model with the gap sensing algorithm, the unscented Kalman filter (UKF) [15] is employed. Finally, we show the simulation results.

2. Mathematical model

2.1 Electromagnetic levitation system

We consider a one-degree of freedom electromagnetic levitation system shown in Fig. 1. The system is stabilized to control the voltage applied to the electromagnet. We assume that the fringing effect is neglected and the permeability of the magnetic material is constant, the flux density is uniformly distributed across the air gap and the leakage flux is neglected to derive the simple model. We will consider magnetic saturation in the sections 3. Then the system can be described by:

$$M\frac{d^2}{dt^2}x = \frac{1}{\mu_0 A}\phi^2 - Mg + F \tag{1}$$

$$v = Ri + N\frac{d}{dt}\phi \tag{2}$$

$$Ni = \frac{1}{\mu_0 A}\left(2x + \frac{l}{\mu_r}\right)\phi \tag{3}$$

where x is the gap, M the mass, g the gravity acceleration, v the input voltage, i the coil current, R the resistance, l the average length of the iron core in the magnetic circuit, μ_0 the permeability of free space, μ_r the relative permeability of the iron core, A the cross sectional area, N the number of coil turns, ϕ the flux of the gap.

2.2 Amplitude modulation approach and demodulation algorithm

Figure 2 shows the concept of the applied voltage v scheme of the amplitude modulation approach. The voltage v consists of the control voltage v_l and the high frequency injection voltage v_h, and accordingly the resulting current i consists of the control current i_l and the high frequency injection current i_h, i.e., $v = v_l + v_h$, $i = i_l + i_h$. Using Eq. (2) and (3), a simplified inductor model of the electromagnet is derived:

$$v = Ri + \frac{d}{dt}\{L(x)i\} \tag{4}$$

where coil inductance

$$L(x) = \mu_0 AN^2\left(2x + \frac{l}{\mu_r}\right)^{-1} \tag{5}$$

We only consider the high frequency components and if the coil resistance R is assumed to be sufficiently small and the frequency of the air gap variation is significantly smaller than the injection frequency, then the Eq. (5) can be expressed as

$$v_h = L(x)\frac{d}{dt}i_h \tag{6}$$

If the injected voltage

$$v_h = V_m\cos(\omega_h t) \tag{7}$$

the excited current i_h can be expressed as:

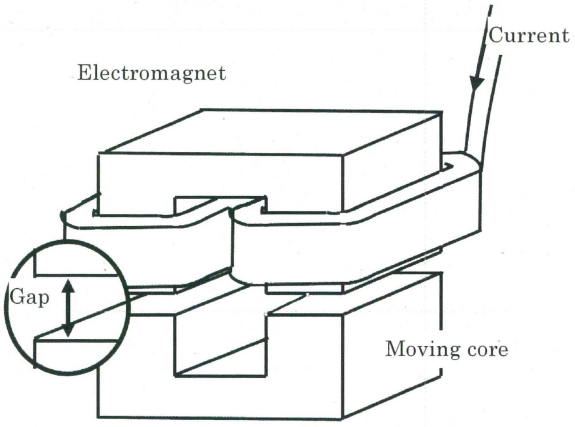

Fig. 1 Electromagnetic Levitation System

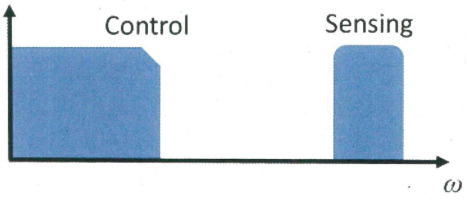

Fig. 2 Frequency spectrum of the voltage

$$i_h = I_m\sin(\omega t) \tag{8}$$

where the current amplitude $I_m = V_m(L(x)\omega)^{-1}$. Using Eqs. (7) and (8), the air gap can be expressed as

$$x = 0.5\left(\mu_0 AN^2\frac{I_m}{V_m} - \frac{l}{\mu_r}\right) \tag{9}$$

Equation (9) shows that the air gap depends on the current amplitude I_m and voltage amplitude V_m.

Next, we show the demodulation algorithm. The square of the current i_h

$$i_h^2 = (I_m\sin(\omega t))^2$$

$$= \frac{1}{2}I_m^2(1 - \cos(2\omega t)) \tag{10}$$

After the low-pass filtering to eliminate the second term of eq. (10), we have

$$LPF\left(i_s^2\right) = \sqrt{\frac{1}{2}}I_m \tag{11}$$

Figure 3 shows the block diagram of the demodulation algorithm. In the algorithm, the control current is approximated by the average current.

2.3 Unscented Kalman filter

The unscented Kalman filter (UKF) is categorized in a class of nonlinear filtering. The UKF uses unscented transform to approximate a probability distribution. The transform removes the requirement to calculate the Jacobian and calculate the sigma points. We consider the following discrete nonlinear system.

$$x_{k+1} = f(x_k) + w_k \tag{12}$$

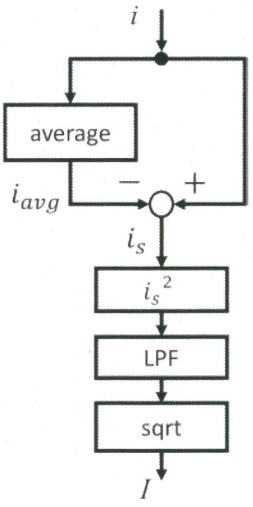

Fig. 3 Amplitude demodulation scheme

$$y_k = h(x_k) + v_k \tag{13}$$

where $x_k \in \Re^n$ is the state at k, $y_k \in \Re^p$ the output at k, $w_k \in \Re^n$ white noise with the covariance Q_k, $v_k \in \Re^p$ the white noise with the covariance R_k, $f : \Re^n \to \Re^n$, $h : \Re^n \to \Re^p$. The UKF algorithm is described as follows:

Step 0. Initialization step at $k = 0$

$$\hat{x}_{0/-1} = \hat{x}_0, P_{0/-1} = P_0$$

Step 1. Calculate the sigma points

$$\hat{x}^0_{k/k} = \hat{x}_{k/k}, W^0 = \frac{\lambda}{n+\lambda}$$

$$\hat{x}^i_{k/k} = \hat{x}_{k/k} + \left(\sqrt{(n+\lambda)P_{k/k}}\right)_i, W^i = \frac{0.5}{n+\lambda}$$

$$\hat{x}^{i+n}_{k/k} = \hat{x}_{k/k} - \left(\sqrt{(n+\lambda)P_{k/k}}\right), W^i = \frac{0.5}{n+\lambda}, i = 1, \cdots, n$$

Step 2. Propagation of the sigma points

$$\hat{x}^i_{k+1/k} = f\left(\hat{x}^i_{k/k}\right), i = 1, \cdots, 2n$$

$$\hat{x}_{k+1/k} = \sum_{i=0}^{2n} W^i \hat{x}^i_{k+1/k}$$

$$P_{k+1/k} = \sum_{i=0}^{2n} W^i \left(\hat{x}^i_{k+1/k} - \hat{x}_{k+1/k}\right)\left(\hat{x}^i_{k+1/k} - \hat{x}_{k+1/k}\right)^T + Q$$

Step 3. Update of the output

$$\hat{y}^i_{k+1/k} = h\left(\hat{x}^i_{k+1/k}\right), i = 1, \cdots, 2n$$

$$\hat{y}_{k+1/k} = \sum_{i=0}^{2n} W^i \hat{y}^i_{k+1/k}$$

Step 4. Calculate the cross covariance matrix

$$V_{k+1/k} = \sum_{i=0}^{2n} W^i \left(\hat{y}^i_{k+1/k} - \hat{y}_{k+1/k}\right)\left(\hat{y}^i_{k+1/k} - \hat{y}_{k+1/k}\right)^T + R$$

$$U_{k+1/k} = \sum_{i=0}^{2n} W^i \left(\hat{x}^i_{k+1/k} - \hat{x}_{k+1/k}\right)\left(\hat{y}^i_{k+1/k} - \hat{y}_{k+1/k}\right)$$

Step 5. Calculate the Kalman gain

$$K_{k+1} = U_{k+1/k} V^{-1}_{k+1/k}$$

Step 6. Calculate the estimated state and the covariance

$$\hat{x}_{k+1/k+1} = \hat{x}_{k+1/k} + K_{k+1}\left(y_k - \hat{y}_{k+1/k}\right)$$

$$P_{k+1/k+1} = P_{k+1/k} - U_{k+1/k} V^{-1}_{k+1/k} U^T_{k+1/k}$$

Step 7. Go to Step 1.

3. Simulation results

3.1 Simulation model

In the previous section, the electromagnetic levitation system described by Eqs. -(1), (2) and (3) were expressed based on the assumption that the iron permeability is constant. However the material permeability is not constant and depends on the magnetic flux density. Now we employ a more exact model to consider magnetic saturation. Table 1 summarizes the model parameters. The flow diagram of the model is shown in Fig. 4.

Table 1 Dimensions of simulation test bench

Sinusoidal injection signal frequency	2kHz
Sinusoidal injection signal amplitude	24V
Maximum control current	10A
Maximum air gap length	1mm
Coil turns	120
Coil resistance	0.3Ω
Pole face area	2.24e-4 m^2

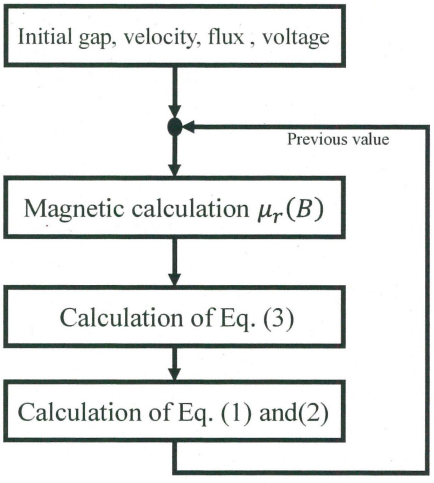

Fig. 4 Flow diagram of the simulation model

3.2 Static characteristics of self-sensing

To investigate the effect of magnetic saturation on the static self-sensing characteristics, we obtained the relationship among the gap length, the current amplitude, and the control current from the simulation results (Fig. 5). In the calculations we varied the gap length from 0.1mm to 0.7mm and the steady state current from 0A to 7A. The current amplitude was calculated by using the algorithm (Fig.3). Figure 5 (a) shows the relationship between the gap length and the current amplitude with different values of the control current. The result shows that the relationship is linear as long as the control current is relatively small. However, if the control current becomes larger, the current amplitude increases significantly. And there is no gap information from the current amplitude and the control current when gap length is 0.5mm and the control current is 4A. Next, Fig. 5 (b) shows the relationship between the control current and the current amplitude with different values of the gap length. The result shows the point where lines intersect exists. The result implies that the gap length is not exactly calculated from the current amplitude and control current.

3.4 Compensation of magnetic saturation

From the simulation result of Fig. 5 in the previous section, the air gap length is not uniquely determined by using the current amplitude and the control current. The non-uniqueness suggests that the additional constraint condition is needed to determine the gap length. One of the conditions is setting the limitation for the solution. If we set that the air gap range 0.6±0.1mm and the maximum current is 3A, the gap can be determined (Fig. 5). In this paper, we utilize the dynamical motion model of the electromagnetic levitation system as the constraint condition. Using Eq. (1), (2) and (3), the discrete dynamical model can be expressed as follows:

$$f(\xi_k)=\begin{pmatrix} \xi_{1k}+h\xi_{2k} \\ \xi_{2k}+h\left\{\dfrac{\mu_0 AN^2}{4M}\left(\dfrac{u}{\xi_{1k}}\right)-g\right\} \end{pmatrix} \tag{14}$$

where x is the gap, v the velocity, $\xi=(x \quad v)^T=(\xi_1 \quad \xi_2)^T$ the state vector, $u=i_l$ the system input.

Using the relationship (Fig. 5), we formulate the observation model with the Lasso regression[16]. The Lasso is a shrinkage and selection method for the linear regression and the L_1- norm regularized least-square regression. We assume that we have the input and output data sets $(x_k, y_k), k=1,2,\cdots n$. And we consider the following function.

$$f(x)=\sum_{k=1}^{n}\alpha_k K(x,x_k) \tag{15}$$

where α_k is an unknown coefficient,

$$K(x,x_k)=\exp\left(-\beta\|x-x_k\|^2\right) \tag{16}$$

, β is the Gauss function parameter. Then we find the parameter such that it minimizes the following function:

$$\sum_{k=1}^{n}(y_k-f(x_j))^T(y_k-f(x_k))+\lambda\sum_{k=1}^{n}|\alpha_k| \tag{17}$$

Where the second term λ is the tuning parameter for the L_1- norm regularization. Using the data set (Fig. 5), we solve the optimization problem and modeled as eq. (15) form. We show the curve fitting result in Fig. 6. The optimized parameters are $\beta=0.5, \lambda=1.5$.

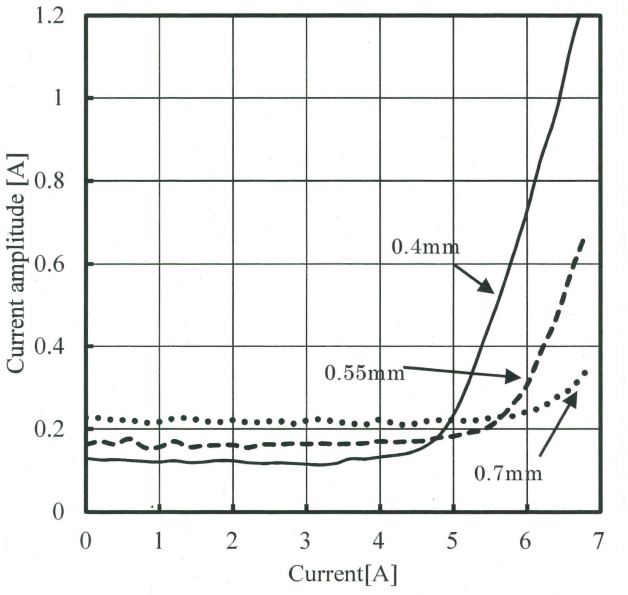

(a) Characteristics of Demodulated signal with respect to current

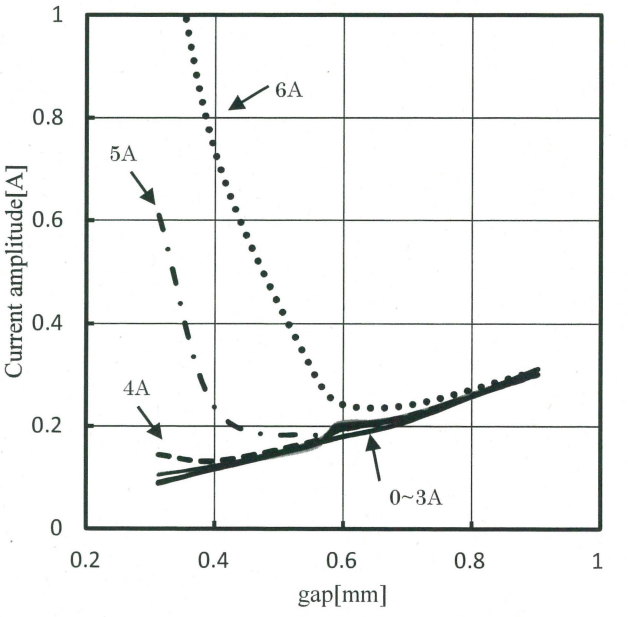

(b) Characteristics of Demodulated signal with respect to gap

Fig. 5. Static characteristics of self-sensing

To incorporate the dynamical model of Eq. (14) with the observation model of Eq. (15), we employ the unscented Kalman filter. Figure 7 shows the proposed the self-sensing system configuration. The coil current are measured and are demodulated by the algorithm (Fig. 3). And the resulting signal are processed by the UKF, which estimate the gap length. Table 2 presents a summary of UKF parameters. Table 3 presents a summary of the controller parameters.

3.5 Self-sensing electromagnetic levitation simulation

When the object is suspended at the steady gap length of 0.5mmm the required steady current 5A. Figure 8 shows the chirp signal response of the air gap length as function of the control current. A chirp signal disturbance is applied to the coil at 0.2 seconds. The signal frequency varies from 0.01Hz to 10Hz. It is expected from the value of

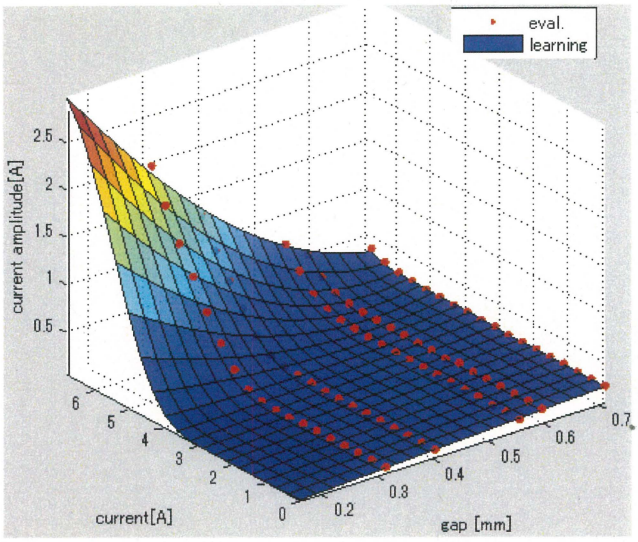

Fig. 6 curve fitting results

the current indicates the iron core is saturated (see Fig. 5). The estimated gap value is coincide with the sensor. The results showed that the gap can be estimated and are controlled while the iron core is saturated.

4. Conclusion

We investigated the magnetic saturation problem of the self-sensing electromagnetic levitation. We showed the relationship among the air gap length, the current amplitude and the control current to confirm the influence of magnetic saturation by using computer simulations. The results showed that the gap is not uniquely estimated when using the relation among the ripple, the control currents and the air gap length. This result implied that it requires additional constraint condition to uniquely identify the gap length. For this problem, we employed the dynamical model of the electromagnetic levitation system and modeled the observation model from the relationship among the ripple and the control currents and the gap length. And we incorporated dynamical model with the observation model by the using unscented Kalman filter (UKF). Finally, we showed that the UKF exactly estimated the gap even if the electromagnet iron core is magnetically saturated. The performance of the proposed self-sensing scheme was demonstrated satisfactorily. Additionally, the performance depends on the accuracy of dynamical model and the observation model. If the parameter variation occurs, the performance of the self-sensing system is deteriorated. However, the number of the dynamical model parameter needs to be identified is only one.

References

1) D. Vischer and H. Bleuler: Self-sensing Active Magnetic Levitation, IEEE Trans. on Magnetics, 29, 2, 92-96 (1993)
2) L. Kucera: Robustness of Self-sensing Magnetic Bearing, in Proceedings of MAG'97 Industrial Conference and Exhibition on Magnetic Bearings, 261-270 (1997)
3) E. Maslen, D. Montie and T. Iwasaki: Robustness limitations in self-sensing magnetic bearings, Journal of Dynamic Systems, Measurement, and Control, 128, 2, 197-203 (2006)

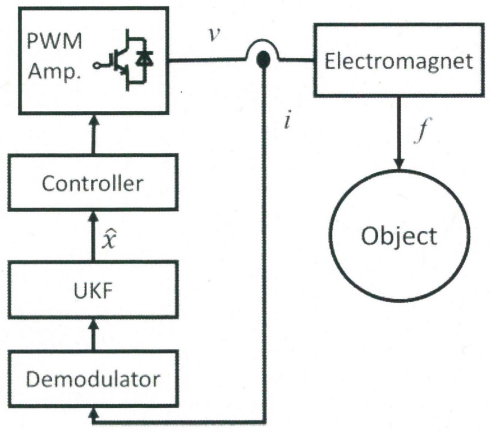

Fig. 7 Proposed self-sensing magnetic levitation system

Table 2 UKF parameters

$\hat{x}_0$	0.5e-3
P_0	Diag(1,1)
Q_k	1e-2
R_k	1e-1
λ	100

Table 3 Controller parameter

Propotional gain	20000
Integral gain	0
Derivative gain	10

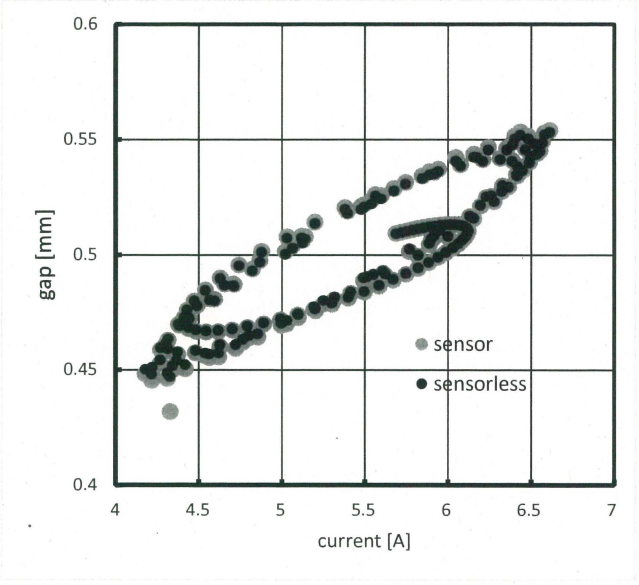

Fig. 8 Chirp signal response

4) N. Morse, R. Smith, B. Paden and J. Antaki: Position Sensed and Self-Sensing Magnetic Bearings Configurations and Associated Robustness Limitations, in Proceedings of the IEEE Conference on Decision and Control Including the Symposium on Adaptive Processes, 3, 2599-2604 (1998)
5) G. van Schoor, A.C. Niemann, and C.P. du Rand: Evaluation of demodulation for robust self-sensing active magnetic bearings,

Sensors and Actuators A: Physical, 189,441-450 (2013)

6) J.S. Yim, S.K. Sul, H.J. Ahn, D.C. Han: Sensorless position control of active magnetic bearings based on high frequency signal injection method, Applied Power Electronics Conference and Exposition, 1, 83-88 (2003)
7) A.H. Ranjbar, R. Noboa and B. Fahimi, Estimation of Airgap Length in Magnetically Levitated Systems, IEEE Trans. on Industry applications, 48, 6, 2173-2181 (2012)
8) T. Gluck, W. Kemmetmuller, C. Tump, A. Kugi: A novel robust postion estimator for self-sensing magnetic levitation systems based on least squares identification, Control Engineering Practice, 19, 2, 146-157 (2011)
9) D. Montie: Performance limitations and self-sensing magnetic bearings, Ph. D. dissertation, University of Virginia, (2003)
10) K.S. Peterson, R.H. Middleton and J.S. Freudenberg: Fundamental Limitaions in Self-Sensing Magnetic Bearings when Modeled as Liniear Periodic Systems, in Proceedings of the American Controls Conference, (2006)
11) A. Schammass, R. Herzog, P. Buhler and H. Bleuler: New Results for Self-sensing Active Magnetic Bearings Using Modulation Approach, IEEE Trans. on Control Systems Technology, 13, 4, 509-516 (2006)
12) K. Matsuda, K. Mito, K. Yamamoto and Y. Okada: Toward the Practical Use of Self-sensing Magnetic Bearing with Nonlinear Compensation, Trans of JSME (C), 72, 723, 3494-3500 (2006)
13) K. Matsumura, T. Yoshida: A New Method for Compensating Current Interference of Self-Sensing Active Magnetic Bearings Using a Bias Source Current Waveform, Trans. IEE of Japan, 129, 5, 526-533 (2009)
14) E.O. Ranft, G. van Schoor and C.P. du Rand: Self-sensing for electromagnetic actuators. Part I: A coupled reluctance network model approach, Sensors and Actuators A: Physical, 172, 441-450 (2011)
15) S.J. Julier and J.K. Uhlmann: A New Extension of the Kalman Filter to Nonlinear Systems, in Proceedings of AeroSense: the 11th International Symposium on Aerospace/Defense Sensing, Simulation and Controls, 182-193 (1997)
16) R. Tibshrani: Regression Shrinkage and Selection via the Lasso, Journal of the Royal Statistical Society Series B, 58, 1, 267-288 (1998)